Supplementary material

On the quest for OER catalysts based on layered double hydroxides: an electrochemical and chemometric combined approach

Isacco Gualandi[1]*, Elisa Musella[1], Giulia Costa[1], Massimo Gazzano[2], Erika Scavetta[1], Sergio Zappoli[1], Domenica Tonelli[1]

[1]University of Bologna, Department of Industrial Chemistry "Toso Montanari", Via Piero Gobetti 85, I-40129 Bologna, Italy.

[2]Istituto per la Sintesi Organica e la Fotoreattività(ISOF), Consiglio Nazionale delle Ricerche (CNR), via Gobetti 101, Bologna, 40129, Italy

Corresponding author: Isacco Gualandi, isacco.gualandi2@unibo.it

SUMMARY

Table S1. Compositions expressed as molar fractions (x) of the LDH tested (in Bold the composition of the verification points)

LABEL	*Co*	*Ni*	*Fe*
A	1.000	0.000	0.000
B	0.800	0.000	0.200
C	0.800	0.200	0.000
D	0.600	0.200	0.200
E	0.600	0.000	0.400
F	0.600	0.400	0.000
G	0.400	0.400	0.200
H	0.400	0.200	0.400
I	0.400	0.000	0.600
J	0.400	0.600	0.000
K	0.200	0.600	0.200
L	0.200	0.200	0.600
M	0.200	0.400	0.400
N	0.200	0.000	0.800
O	0.200	0.800	0.000
P	0.000	1.000	0.000
Q	0.000	0.200	0.800
R	0.000	0.800	0.200
S	0.000	0.400	0.600
T	0.000	0.600	0.400
U	0.165	0.165	0.670
V	0.670	0.165	0.165
W	0.330	0.330	0.330
X	0.165	0.670	0.165

XRD Co LDH

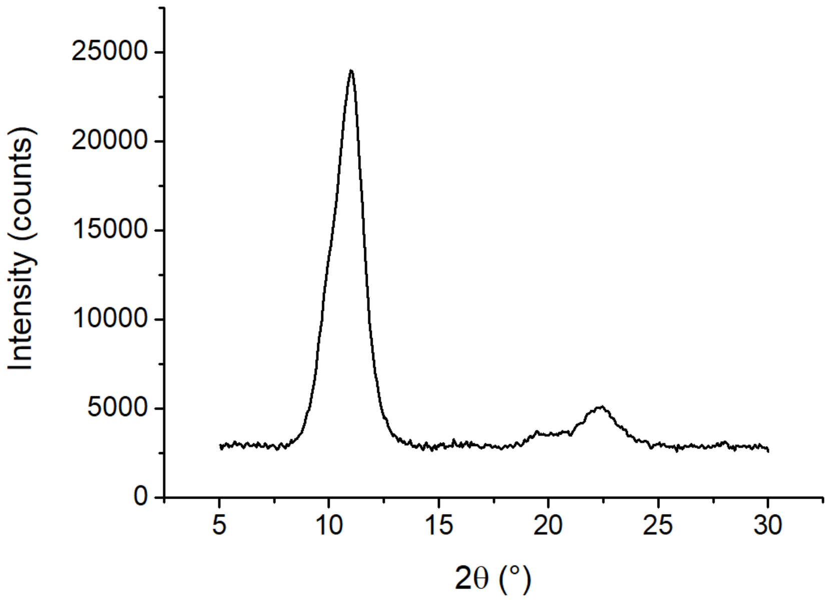

Figure S1. XRD of Co100 LDH (A)

XRD Ni LDH

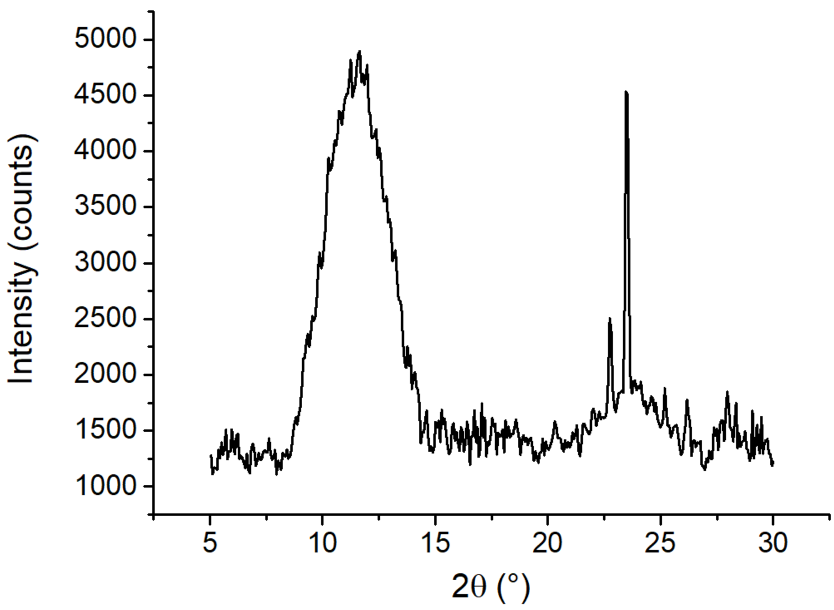

Figure S2. XRD of Ni100 LDH (P)

XRD CoFe LDH

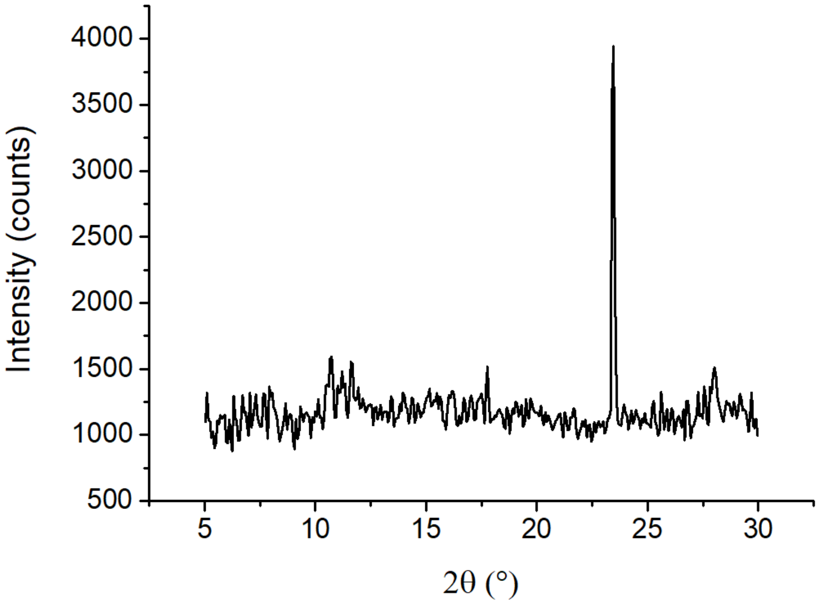

Figure S3. XRD of Co20Fe80 LDH (N)

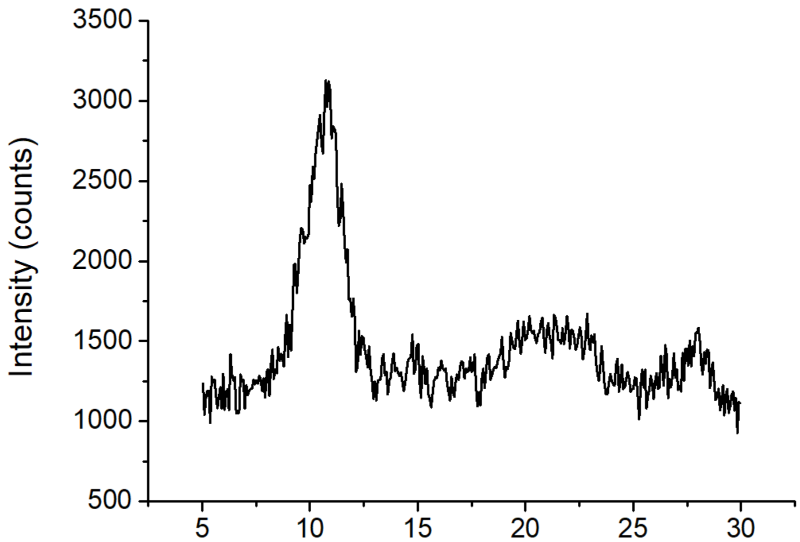

Figure S4. XRD of Co40Fe60 LDH (I)

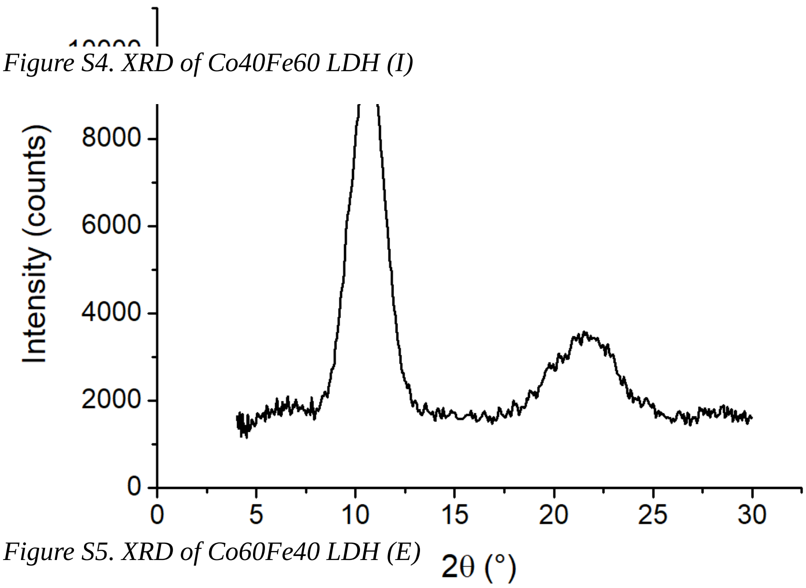

Figure S5. XRD of Co60Fe40 LDH (E)

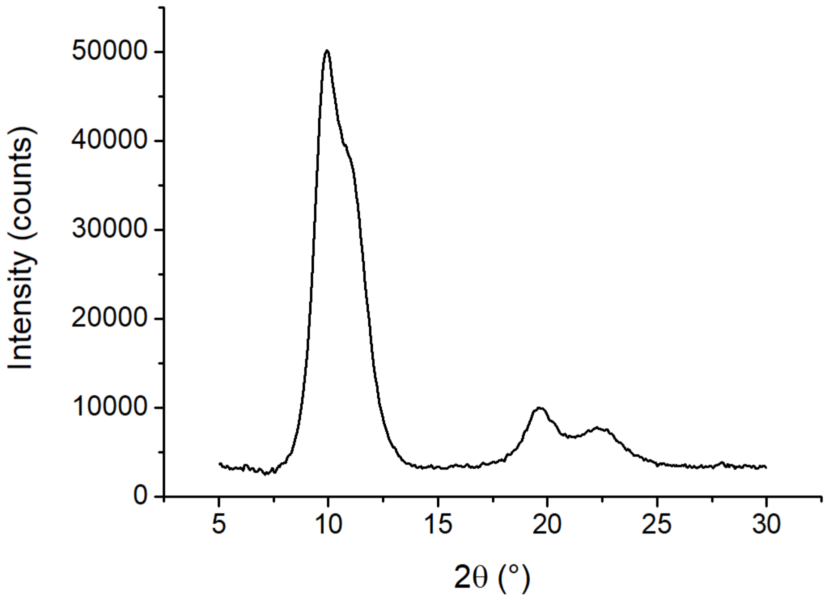

Figure S6. XRD of Co80Fe20 LDH (B)

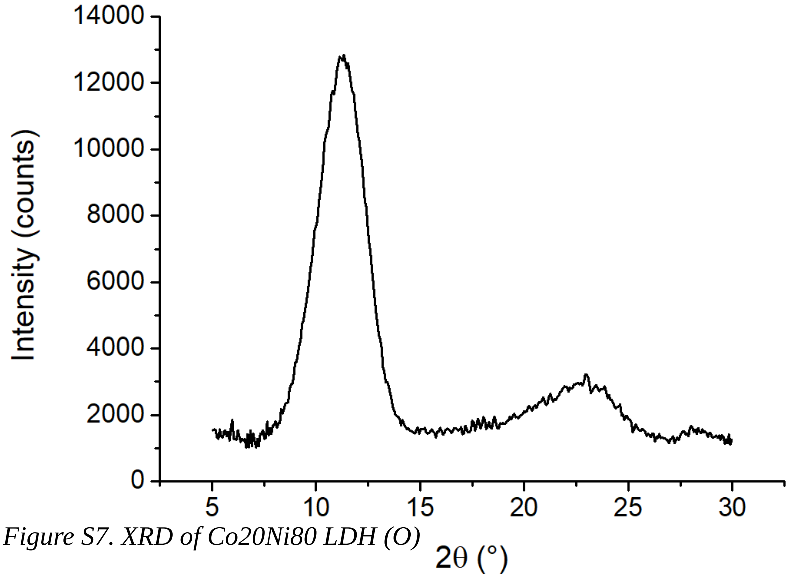

XRD CoNi LDH

Figure S7. XRD of Co20Ni80 LDH (O)

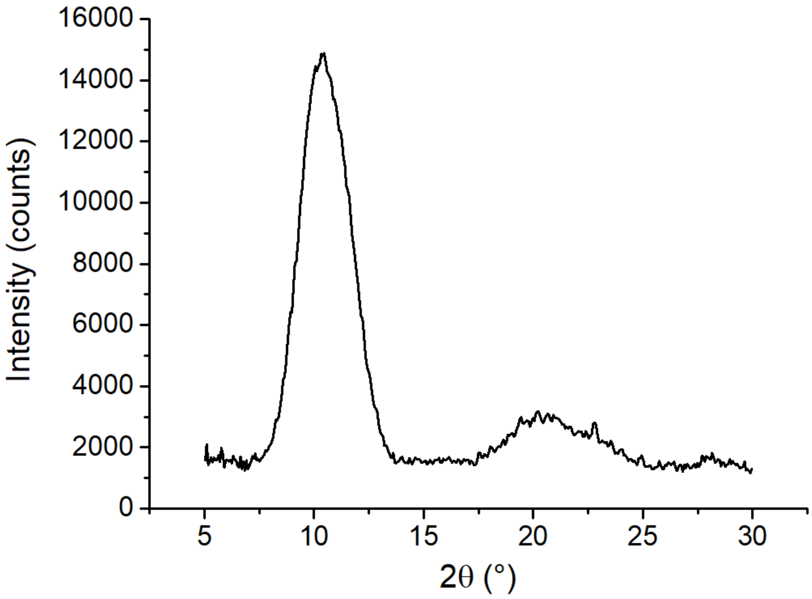

Figure S8. XRD of Co40Ni60 LDH (J)

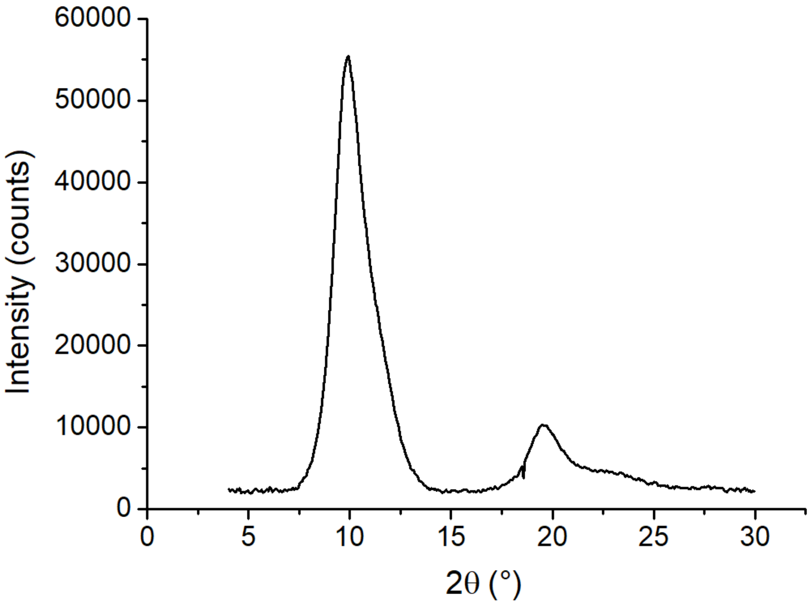

Figure S9. XRD of Co60Ni40 LDH (F)

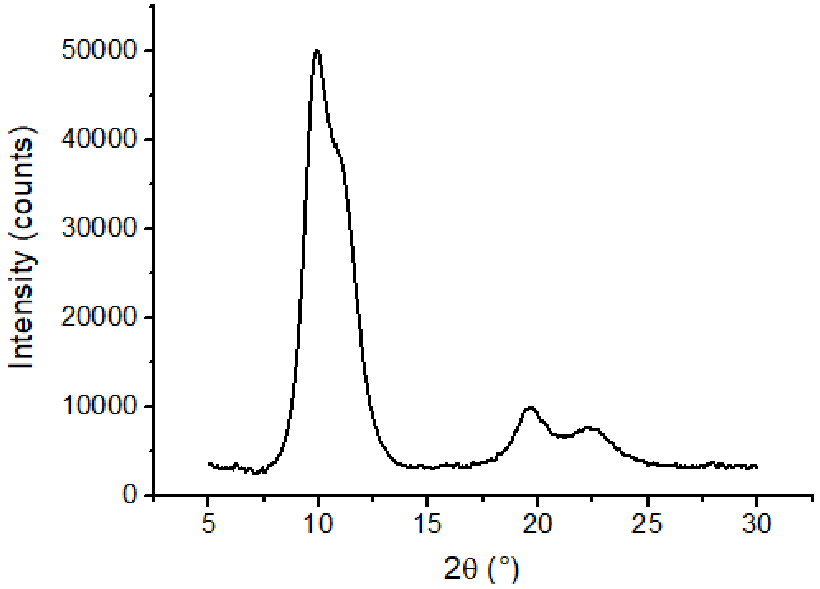

Figure S10. XRD of Co80Ni20 LDH (C)

XRD NiFe LDH

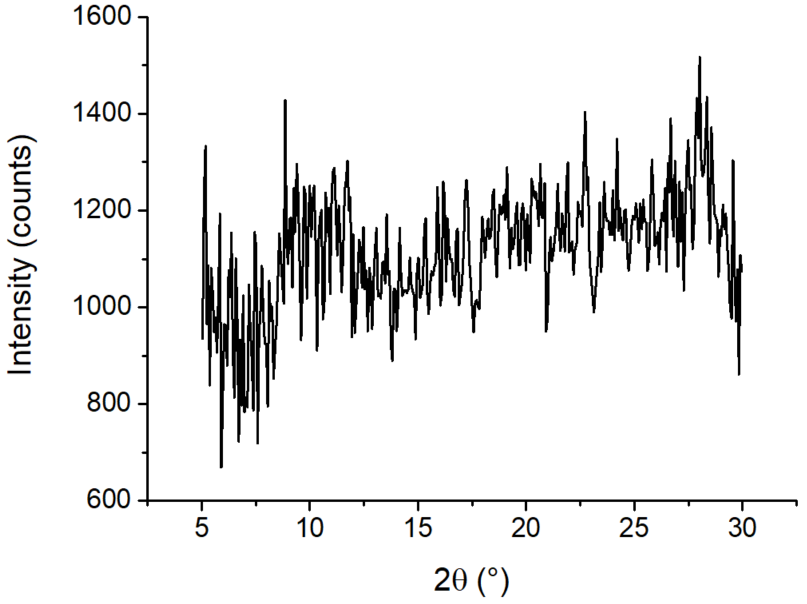

Figure S11. XRD of Ni20Fe80 LDH (Q)

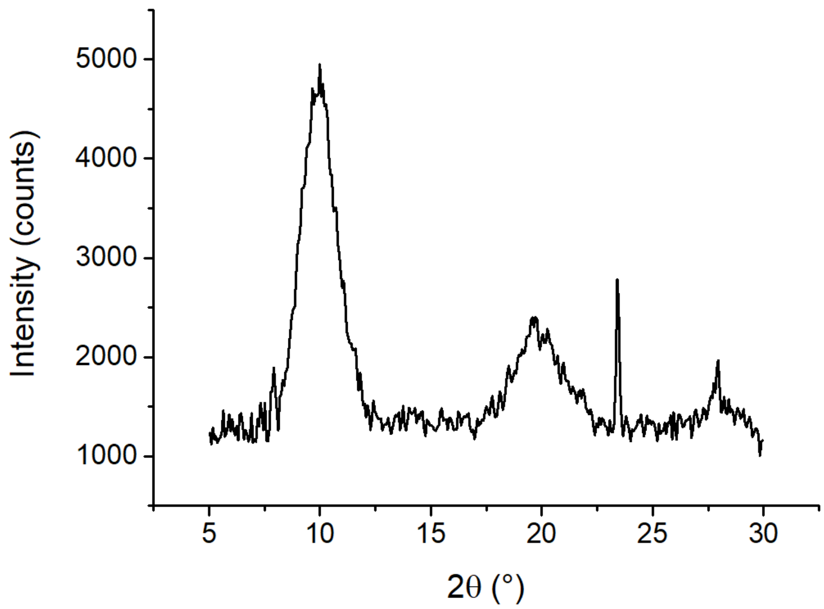

Figure S12. XRD of Ni40Fe60 LDH (S)

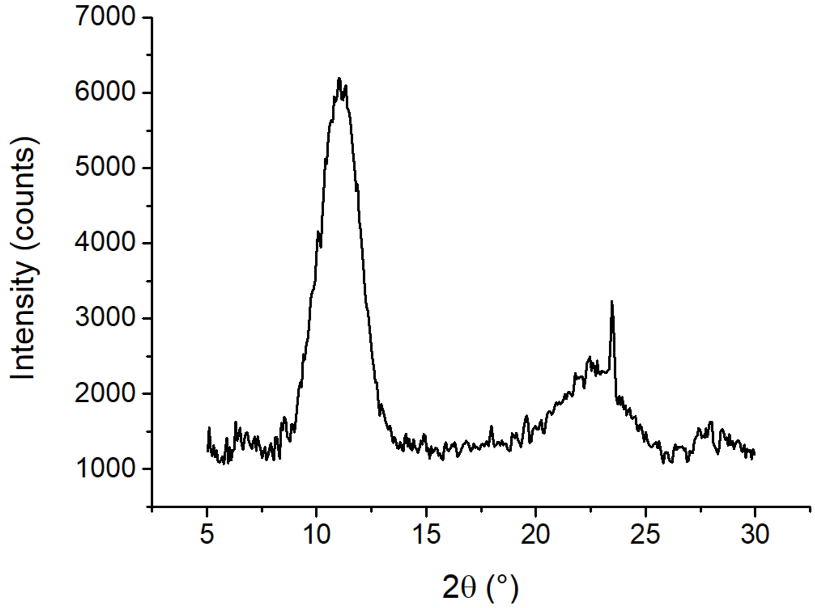

Figure S13. XRD of Ni60Fe40 LDH (T)

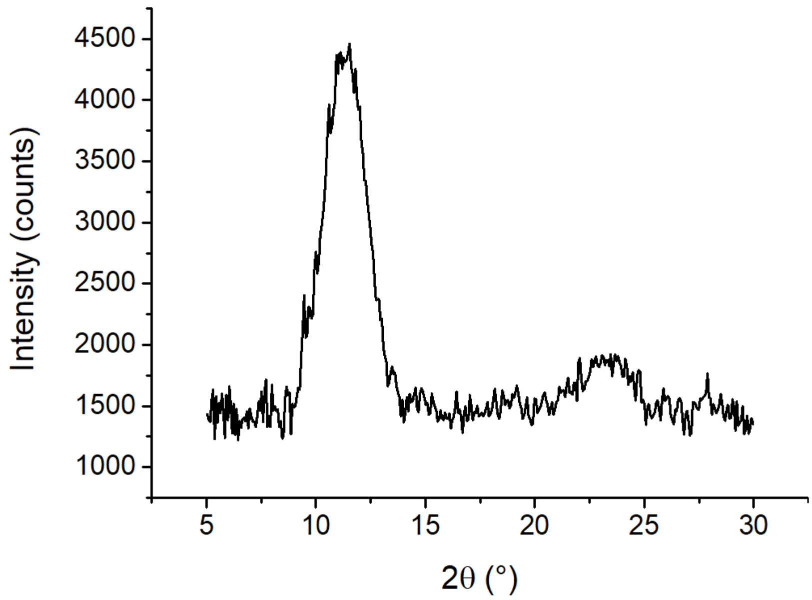

Figure S14. XRD of Ni80Fe20 LDH (R)

XRD CoNiFe LDH

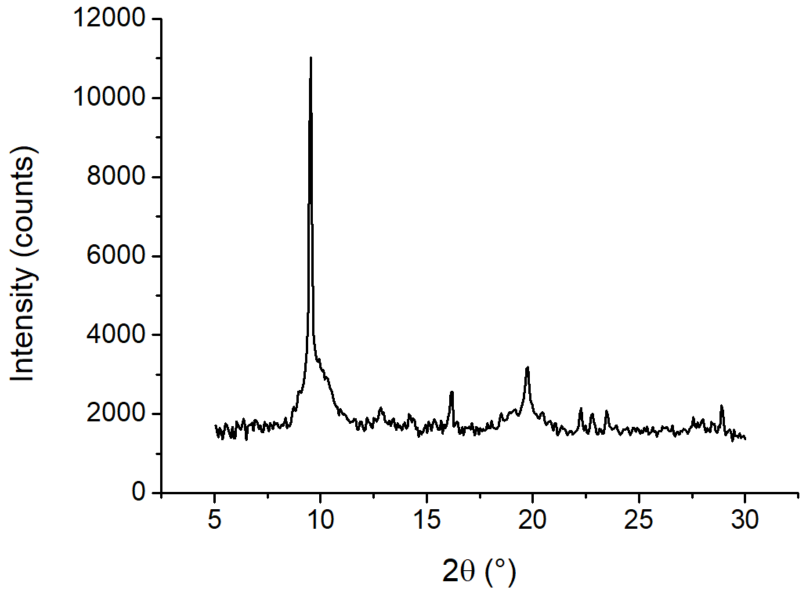

Figure S15. XRD of Co16.5Ni16.5Fe67 LDH (U)

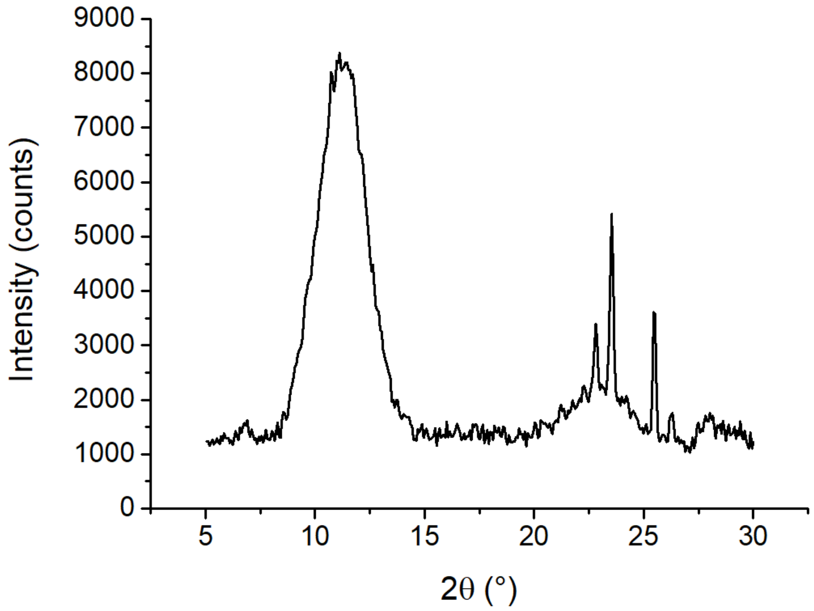

Figure S16. XRD of Co16.5Ni67Fe16.5 LDH (X)

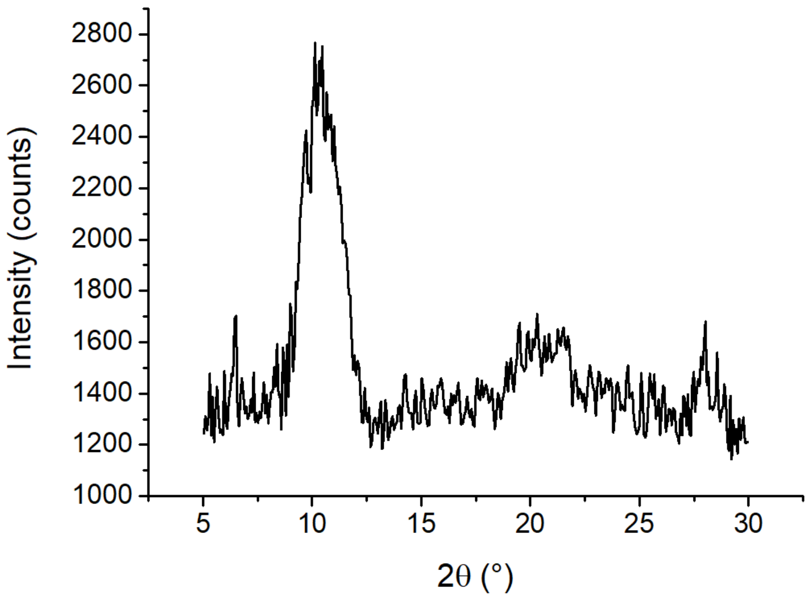

Figure S17. XRD of Co20Ni20Fe60 LDH (L)

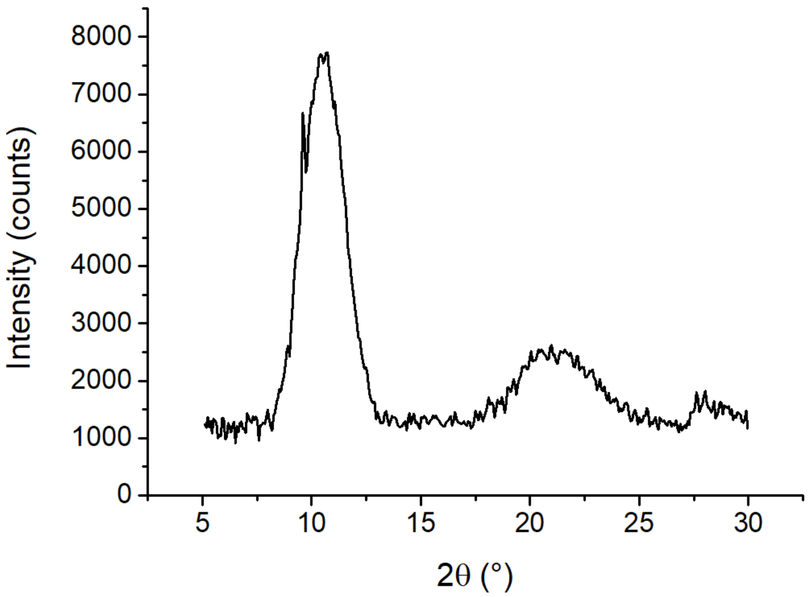

Figure S18. XRD of Co20Ni40Fe40 LDH (M)

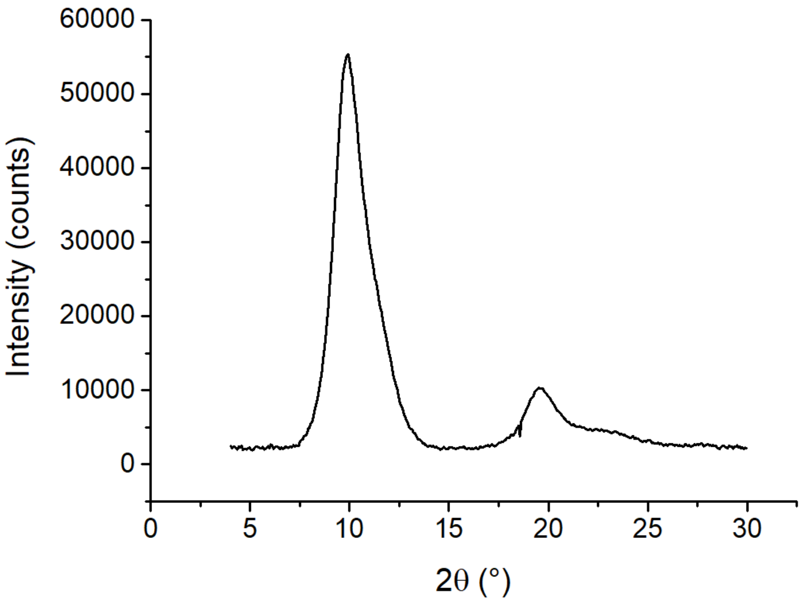

Figure S19. XRD of Co20Ni60Fe20 LDH (K)

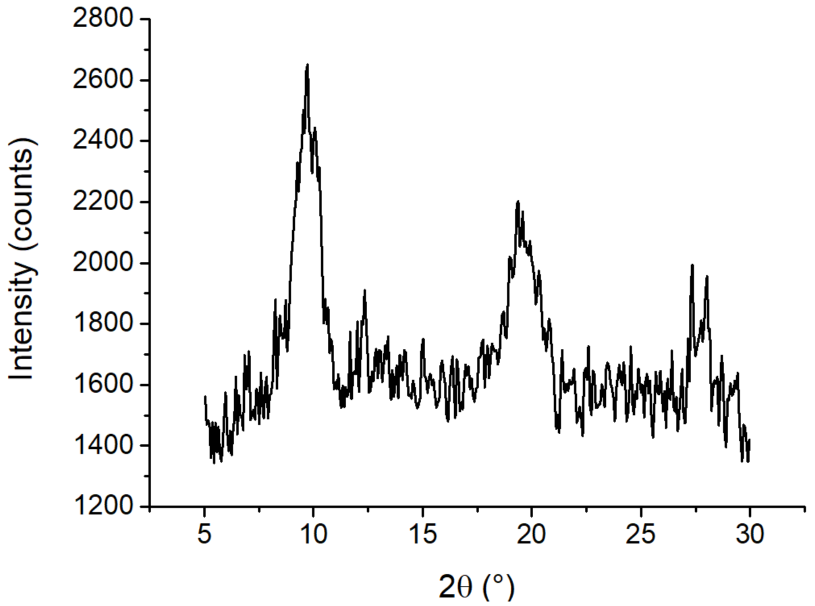

Figure S20. XRD of Co33Ni33Fe33 LDH (W)

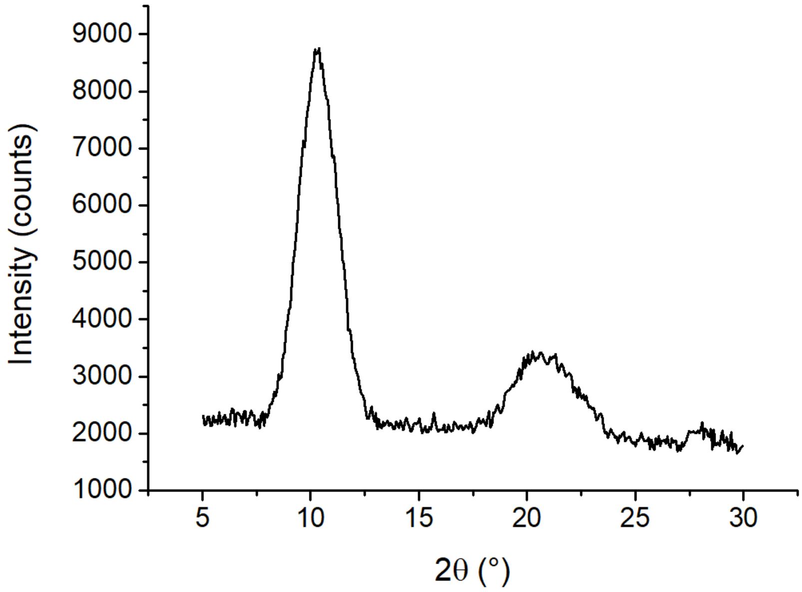

Figure S21. XRD of Co40Ni20Fe40 LDH (H)

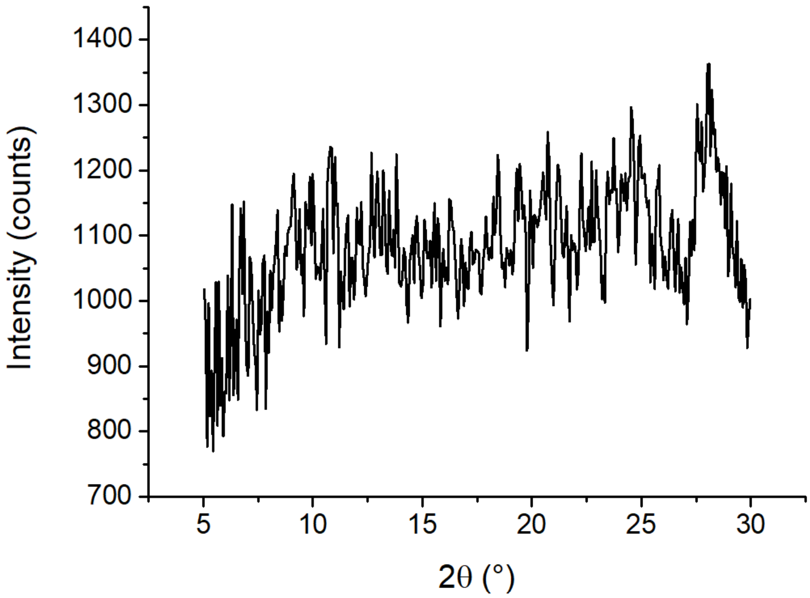

Figure S22. XRD of Co40Ni40Fe20 LDH (G)

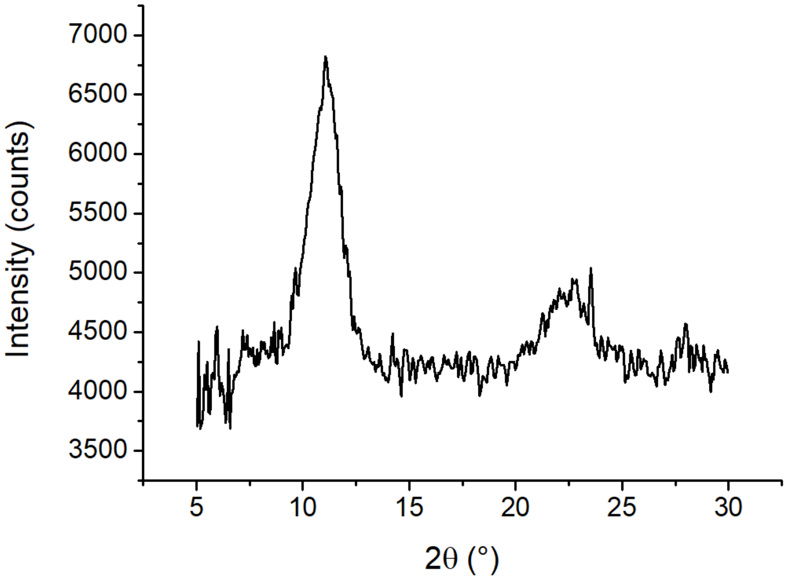

Figure S23. XRD of Co60Ni20Fe20 LDH (D)

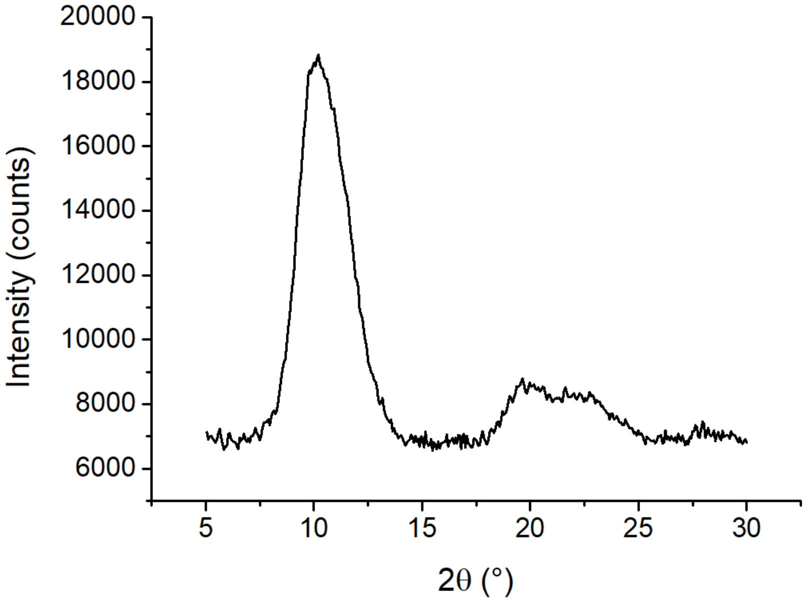

Figure S24. XRD of Co67Ni16.5Fe16.5 LDH (V)

CV CoFe LDH

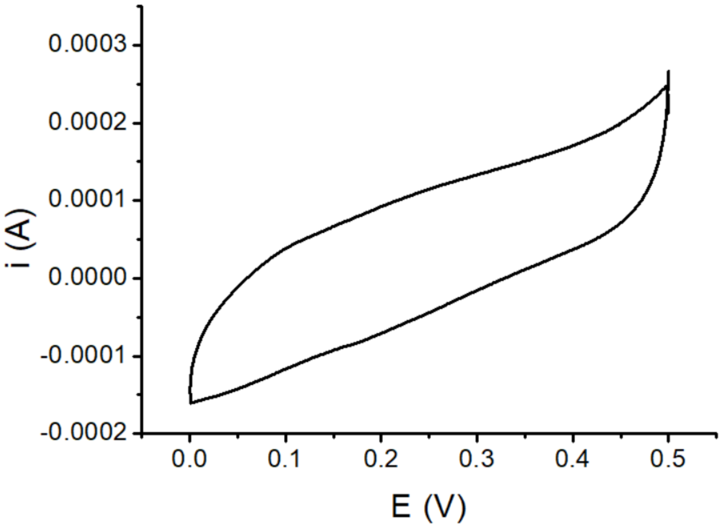

Figure S25. CV of Co20Fe80 (N) LDH recorded in 0.1 M KOH solution; scan rate: 10 mV/s

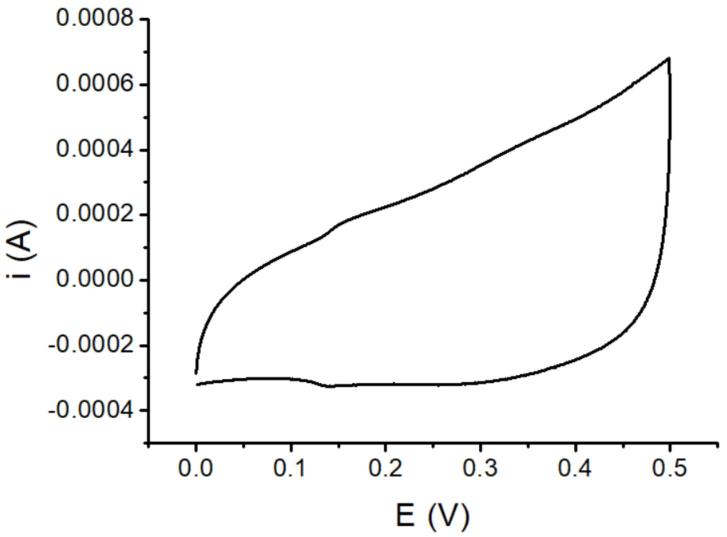

Figure S26. CV of Co40Fe60 (I) LDH recorded in 0.1 M KOH solution; scan rate10 mV/s

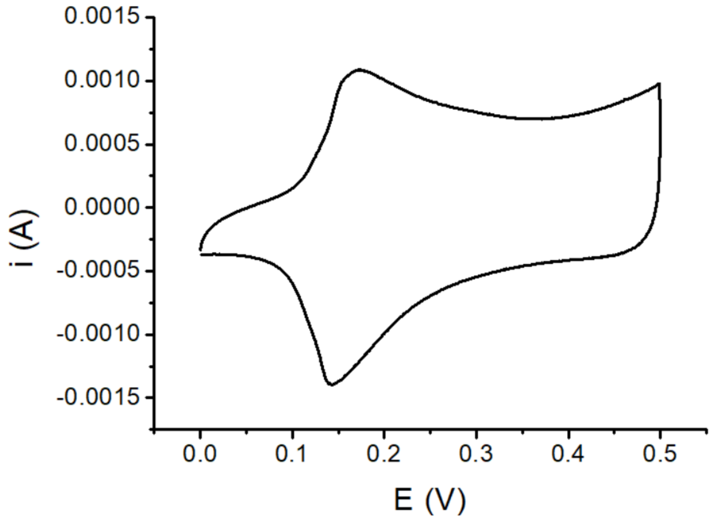

Figure S27. CV of Co60Fe40 (E) LDH recorded in 0.1 M KOH solution; scan rate10 mV/s

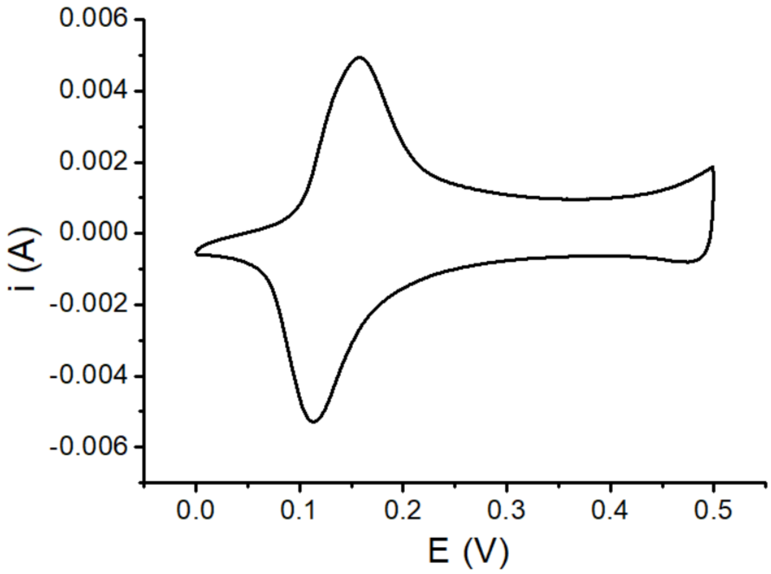

Figure S278. CV of Co80Fe20 (B) LDH recorded in 0.1 M KOH solution; scan rate10 mV/s

CV CoNi LDH

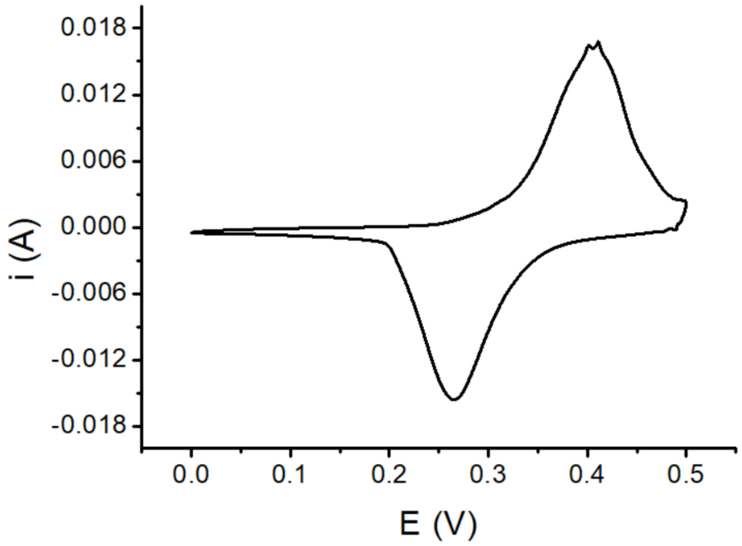

Figure S289. CV of Co20Ni80 (O) LDH recorded in 0.1 M KOH solution; scan rate10 mV/s

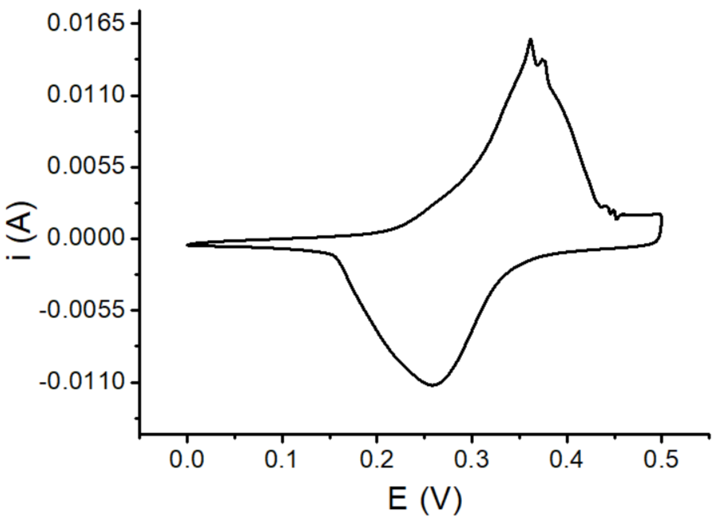

Figure S30. CV of Co40Ni60 (J) LDH recorded in 0.1 M KOH solution; scan rate10 mV/s

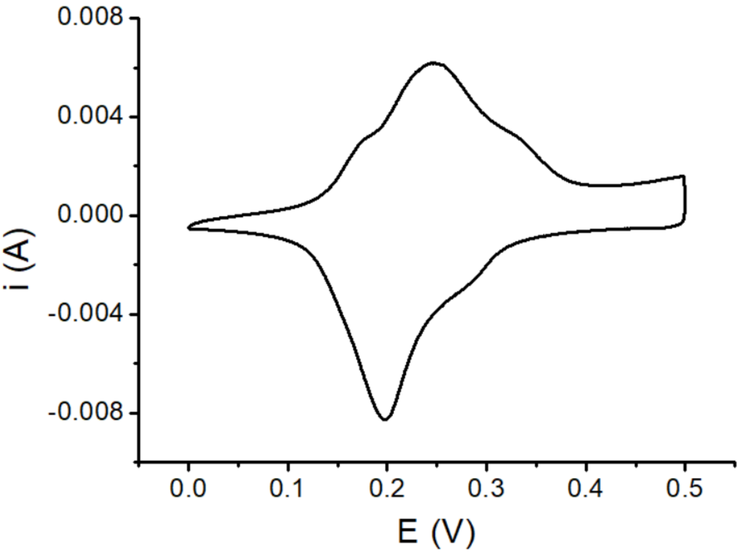

Figure S291. CV of Co60Ni40 (F) LDH recorded in 0.1 M KOH solution; scan rate10 mV/s

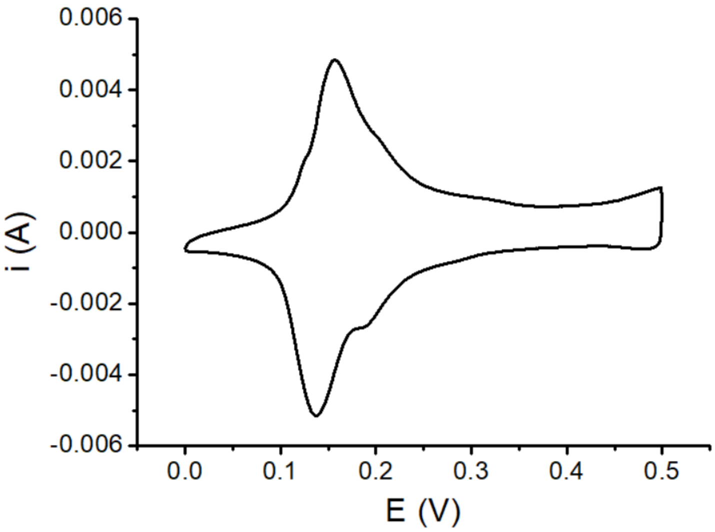

Figure S302. CV of Co80Ni20 (C) LDH recorded in 0.1 M KOH solution; scan rate10 mV/s

CV Co LDH

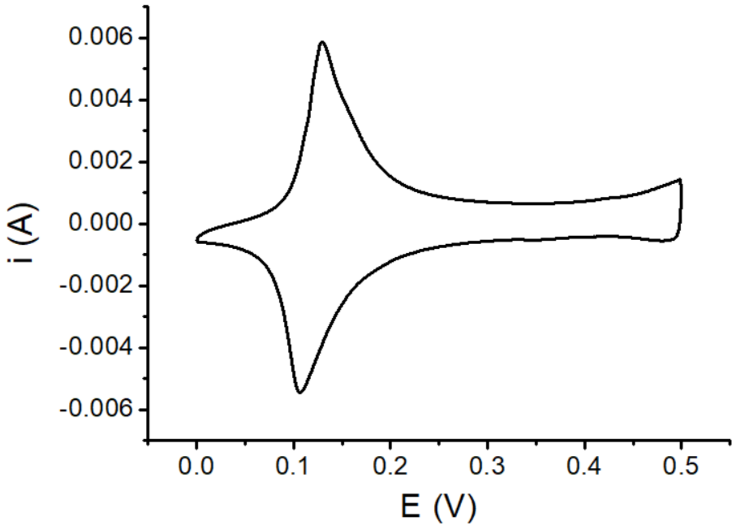

Figure S313. CV of Co100 (A) LDH recorded in 0.1 M KOH solution; scan rate10 mV/s

CV Ni LDH

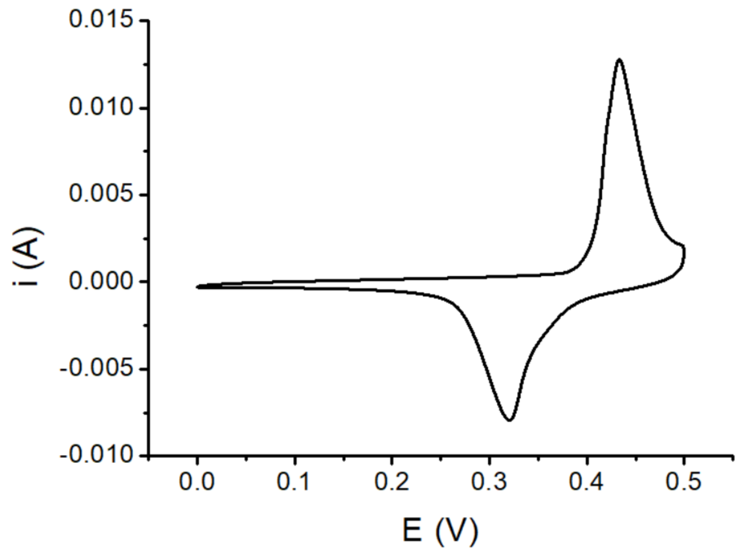

Figure S324. CV of Ni100 (P) LDH recorded in 0.1 M KOH solution; scan rate10 mV/s

CV NiFe LDH

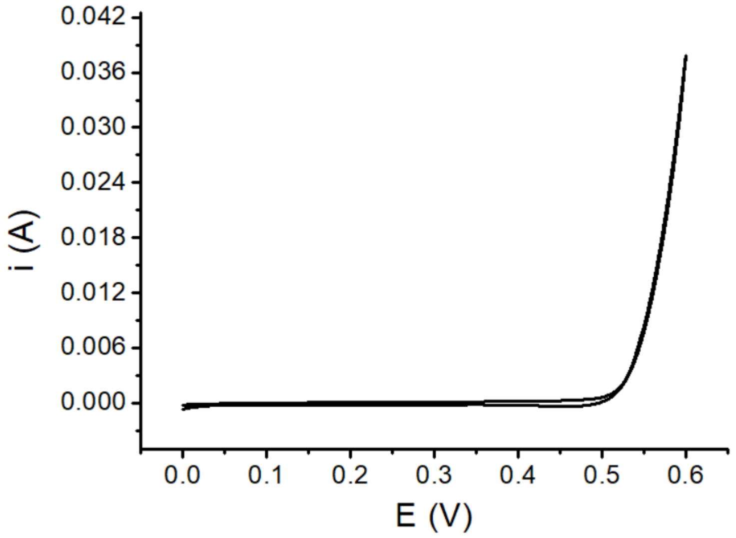

Figure S335. CV of Ni20Fe80 (Q) LDH recorded in 0.1 M KOH solution; scan rate10 mV/s

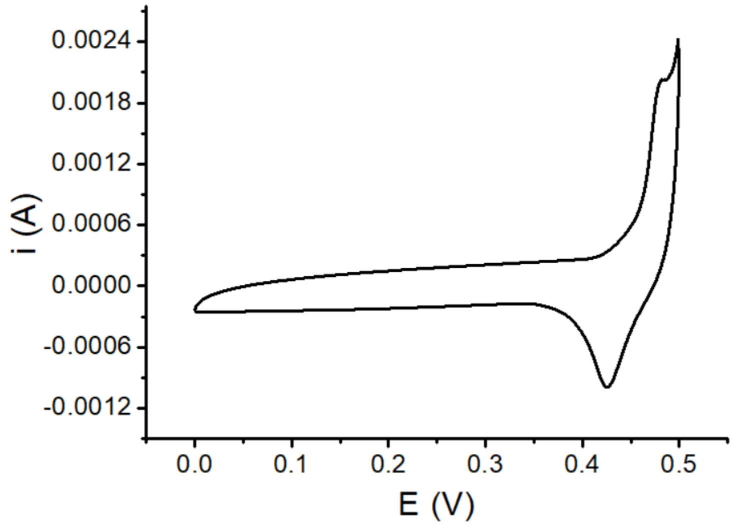

Figure S346. CV of Ni40Fe60 (S) LDH recorded in 0.1 M KOH solution; scan rate10 mV/s

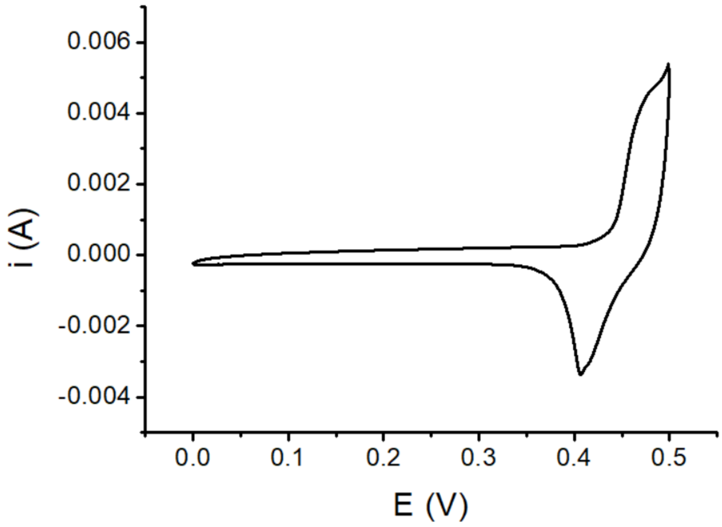

Figure S357. CV of Ni60Fe40 (T) LDH recorded in 0.1 M KOH solution; scan rate10 mV/s

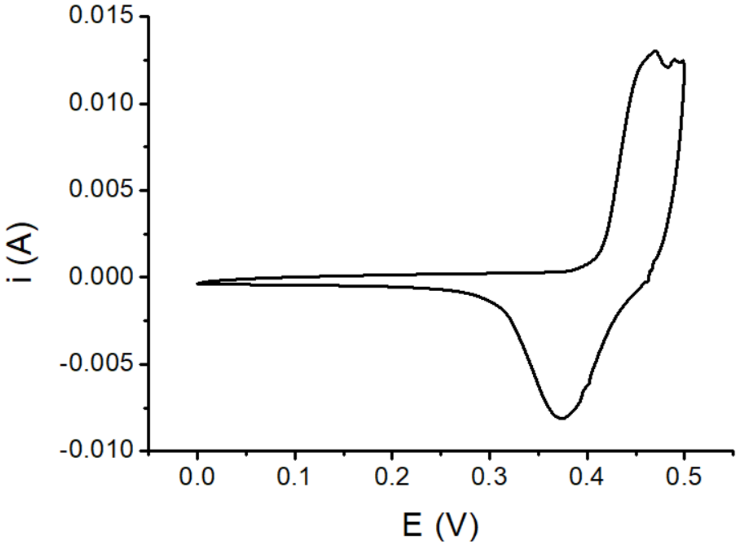

Figure S368. CV of Ni80Fe20 (R) LDH recorded in 0.1 M KOH solution; scan rate10 mV/s

CV CoNiFe LDH

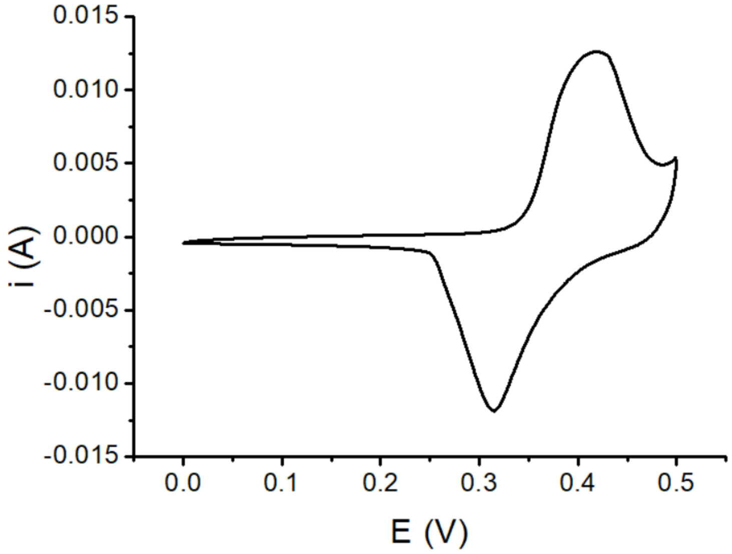

Figure S379. CV of Co16.5Ni67Fe16.5 (X) LDH recorded in 0.1 M KOH solution; scan rate10 mV/s

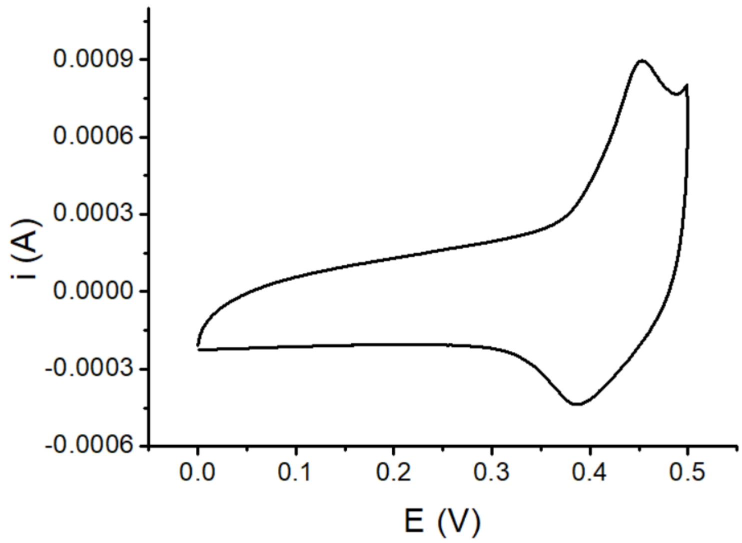

Figure S40. CV of Co16.5Ni16.5Fe67 (U) LDH recorded in 0.1 M KOH solution; scan rate10 mV/s

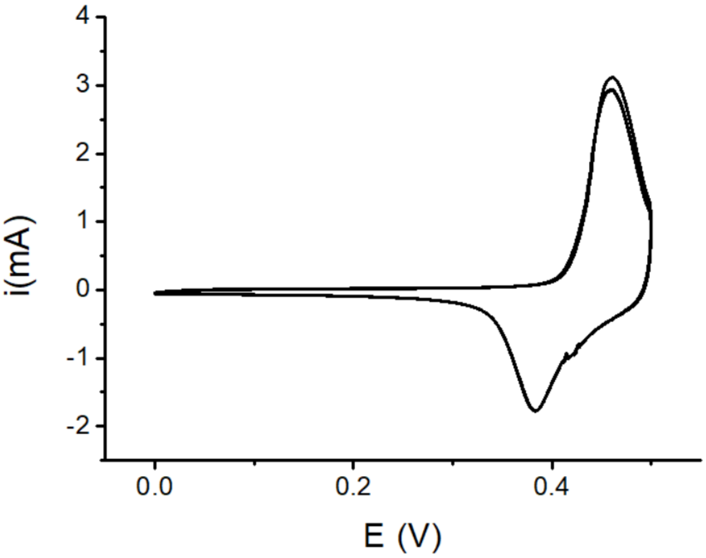

Figure S41. CV of Co20Ni40Fe40 (M) LDH recorded in 0.1 M KOH solution; scan rate10 mV/s

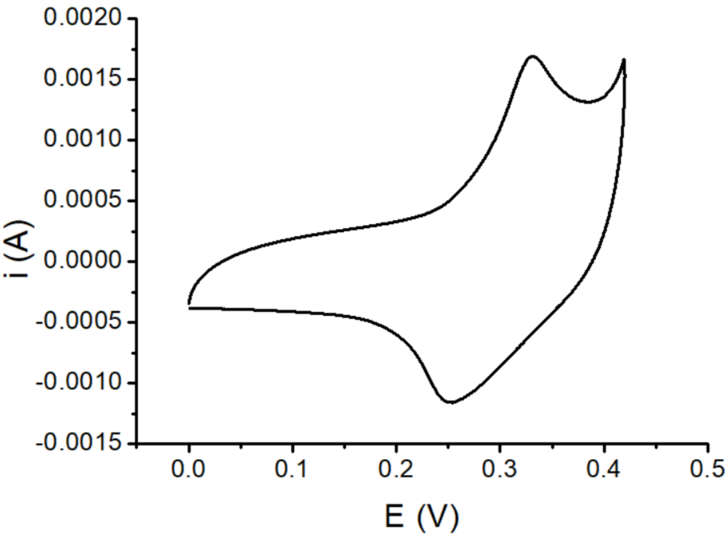

Figure S382. CV of Co20Ni20Fe60 (L) LDH recorded in 0.1 M KOH solution; scan rate10 mV/s

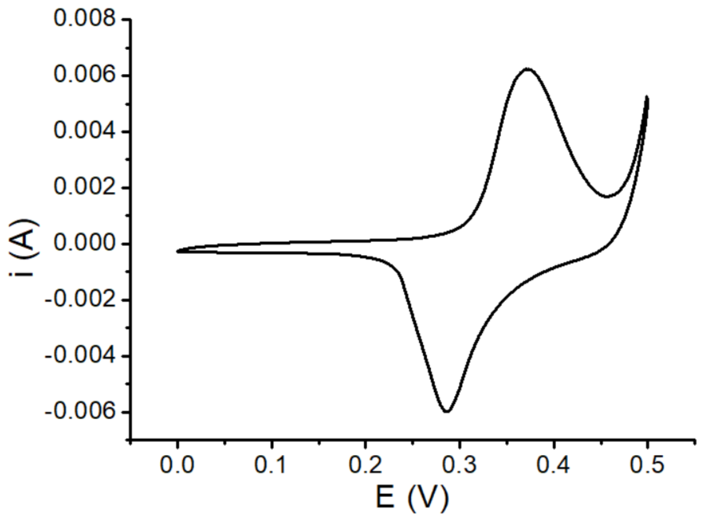

Figure S393. CV of Co20Ni60Fe20 (K) LDH recorded in 0.1 M KOH solution; scan rate10 mV/s

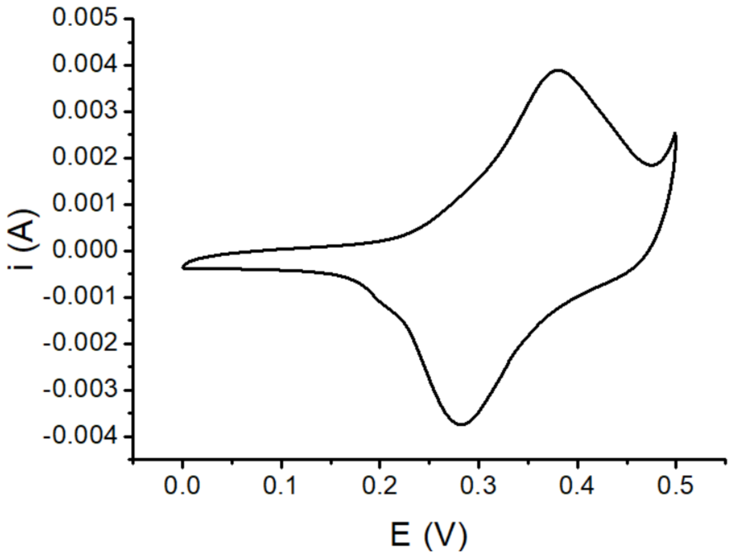

Figure S404. CV of Co33Ni33Fe33 (W) LDH recorded in 0.1 M KOH solution; scan rate10 mV/s

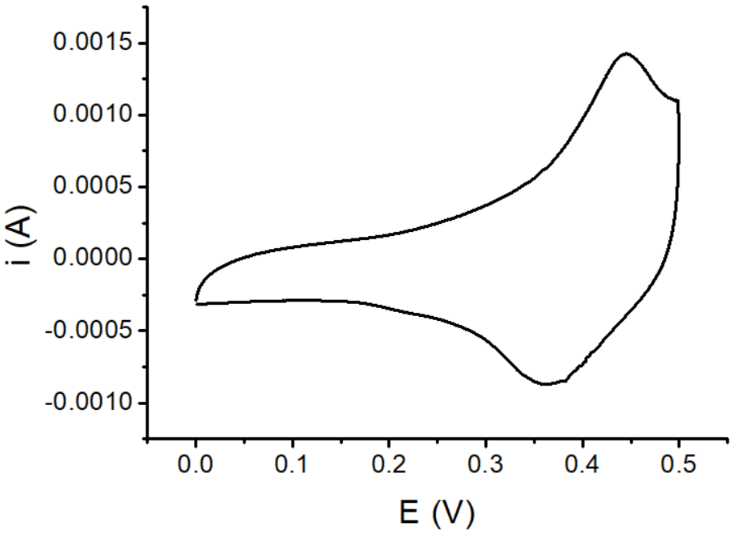

Figure S415. CV of Co40Ni20Fe40 (H) LDH recorded in 0.1 M KOH solution; scan rate10 mV/s

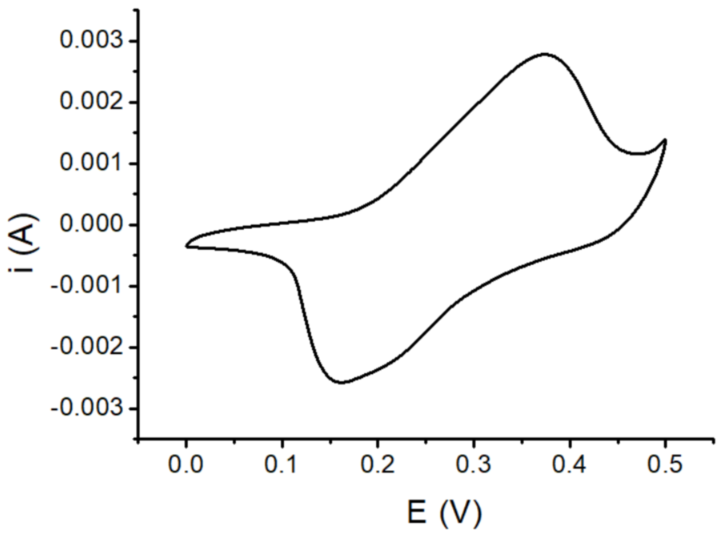

Figure S426. CV of Co40Ni40Fe20 (G) LDH recorded in 0.1 M KOH solution; scan rate10 mV/s

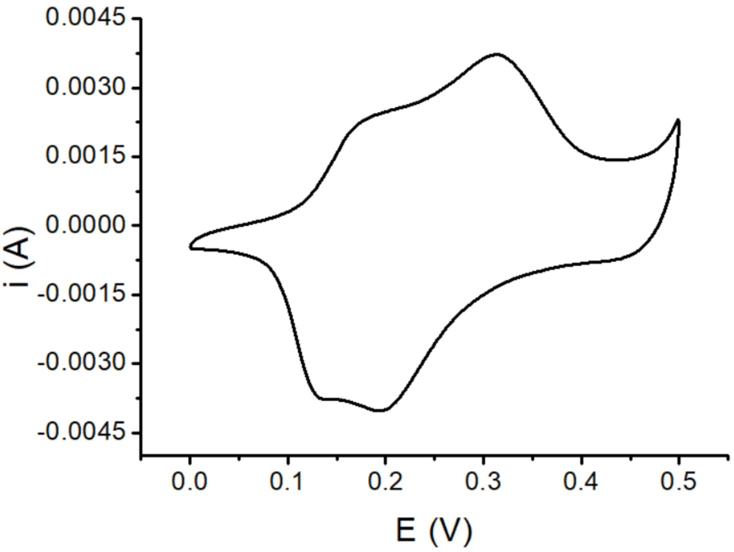

Figure S437. CV of Co60Ni20Fe20 (D) LDH recorded in 0.1 M KOH solution; scan rate10 mV/s

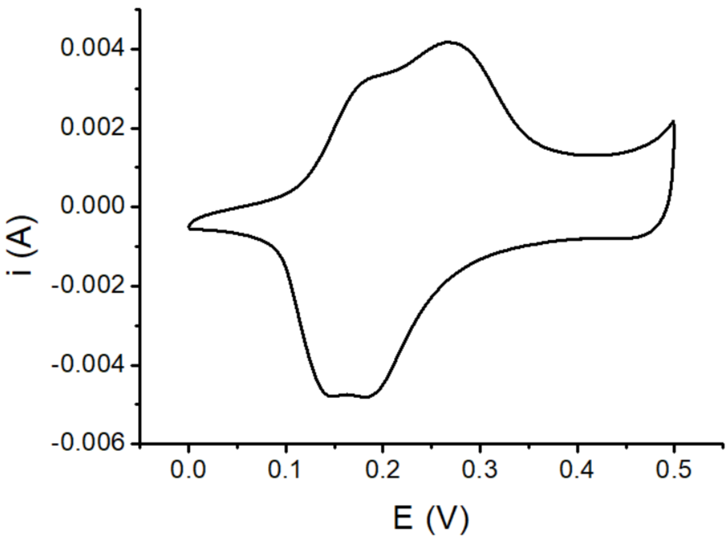

Figure S448. CV of Co67Ni16.5Fe16.5 (V) LDH recorded in 0.1 M KOH solution; scan rate10 mV/s

Table S2. Observed or calculated parameters for the different experiments conducted for the model definition.

LABEL	*#*	*Fract Co*	*Fract Ni*	*Fract Fe*	*Tafel Slope (mV dec-1)*	*Eonset (V vs RHE)*	*Over-potential* (V)*	*Ip (A)*	*Ep (V vs SCE)*	*cryst size (Å)*
A	1	1	0	0	142.0	1.550	0.321	0.00640	0.129	59.9
B	2	0.8	0	0.2	86.0	1.504	0.257	0.00498	0.154	41.6
C	3	0.8	0.2	0	124.0	1.560	0.331	0.00486	0.156	68.8
D	4	0.6	0.2	0.2	62.9	1.469	0.240	n.d.	0.267	50.7
E	5	0.6	0	0.4	87.0	1.523	0.294	0.00110	0.225	43.3
F	6	0.6	0.4	0	120.0	1.555	0.326	0.00510	0.228	52.2
G	7	0.4	0.4	0.2	59.1	1.493	0.264	0.00683	0.322	40.3
H	8	0.4	0.2	0.4	77.4	1.483	0.254	0.00218	0.348	42.6
I	9	0.4	0	0.6	77.0	1.532	0.303	n.d.	nd	44.3
J	10	0.4	0.6	0	134.0	1.553	0.324	0.01400	0.370	33.6
K	**11**	0.2	0.6	0.2	53.2	1.505	0.276	n.d.	0.387	41.8
L	12	0.2	0.2	0.6	97.0	1.510	0.281	0.00078	0.515	39.2
M	13	0.2	0.4	0.4	66.8	1.501	0.272	0.00218	0.403	44.8
N	14	0.2	0	0.8	62.0	1.556	0.327	n.d.	n.d.	n.d.
O	15	0.2	0.8	0	136.0	1.559	0.330	0.01700	0.403	33.1
P	16	0	1	0	188.0	1.564	0.335	0.01020	0.442	28.1
Q	17	0	0.2	0.8	56.0	1.510	0.281	n.d.	n.d.	n.d.
R	18	0	0.8	0.2	233.0	1.551	0.322	0.01240	n.d.	38.7
S	**19**	0	0.4	0.6	70.0	1.488	0.259	0.00088	0.477	47.2
T	20	0	0.6	0.4	213.0	1.557	0.328	0.00888	0.475	41.3

**the overpotetial is calculated by reporting the E_{onset} with respect to the potentials of $1/2O_2/H_2O$ couple in 0.1 M KOH*

Table S3. Standardized main effects of factors on the studied responses. Interaction effects are always not significant

	Std. Effect			***Std** Effect %*			
	Ni	**Co**	**Fe**	**Ni**	**Co**	**Fe**	**Total effect**
TAFEL	**6.8**	**4.4**	2.0	**41.4**	**27.1**	12.4	80.89 %
E_OnSet	**89.4**	**87.4**	**50.5**	**38.5**	**37.7**	**21.7**	97.86 %
Ip	**5.5**	2.0	0.6	**55.8**	20.3	6.2	82.24 %
Ep	**15.1**	**3.4**	**6.0**	**52.4**	**11.7**	**20.7**	84.79 %
CrySize	**5.6**	**13.4**	**3.1**	**22.5**	**53.7**	**12.4**	88.58 %

Legend. Marked effects are significative (p >0.05)

Pareto charts

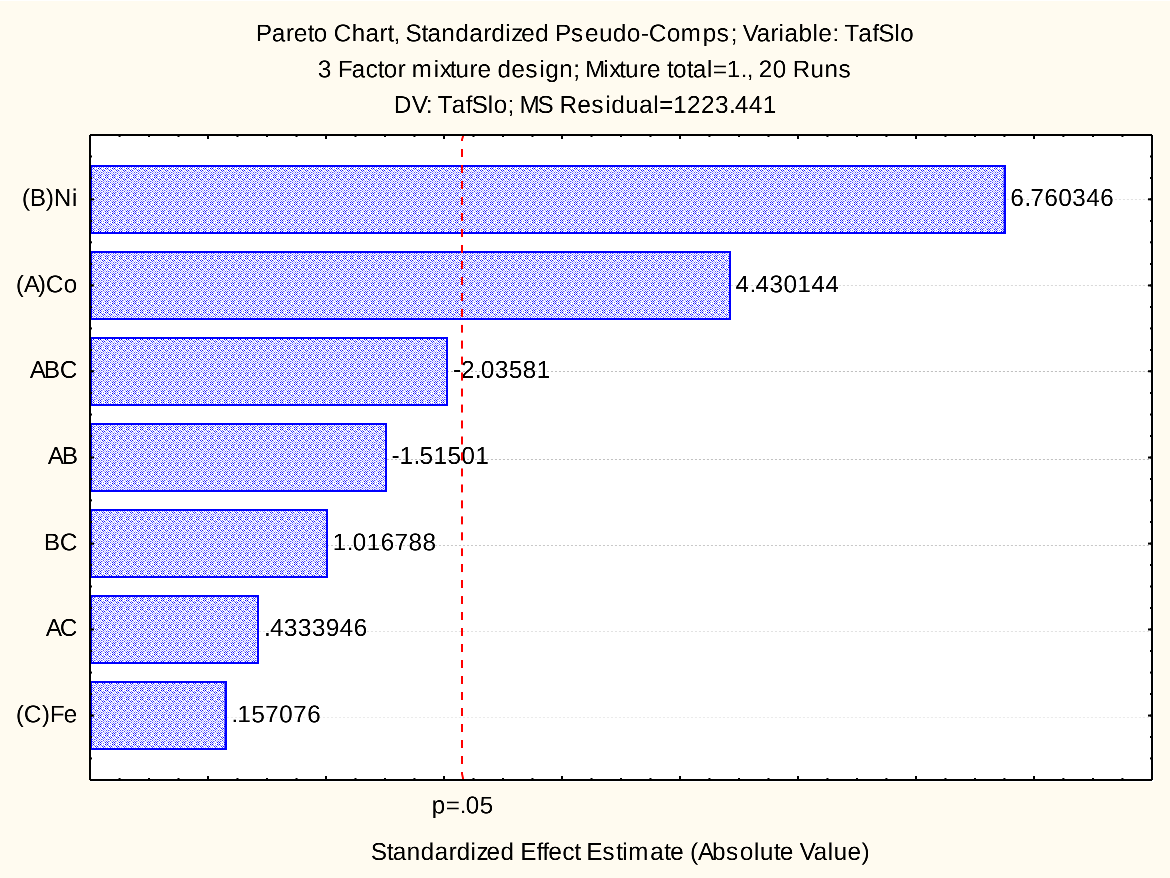

Figure S49. Pareto chart of Tafel slope

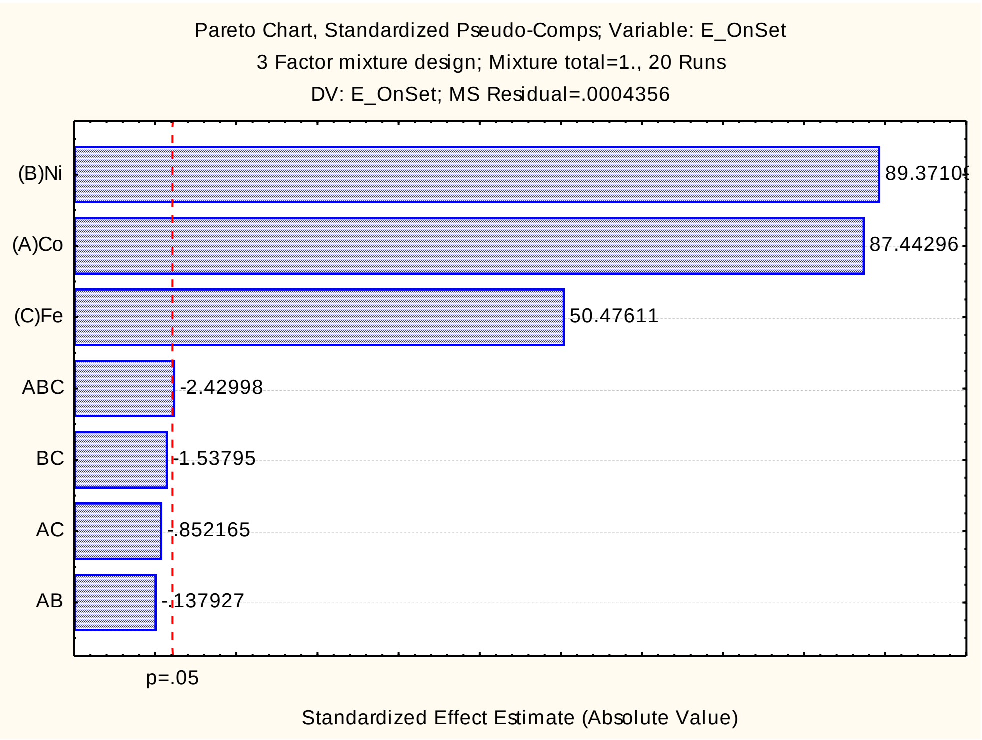

Figure S50. Pareto chart of E_{onset}

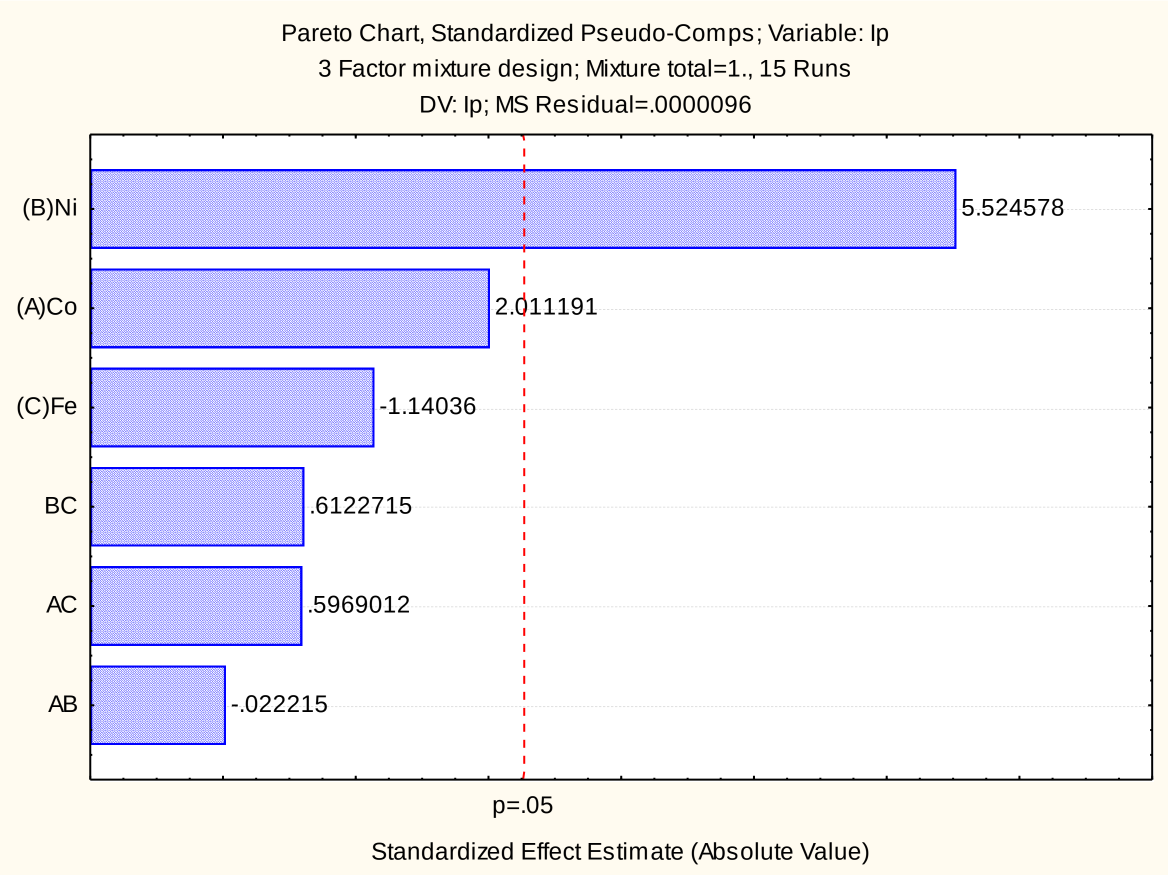

Figure S51. Pareto chart of I_p

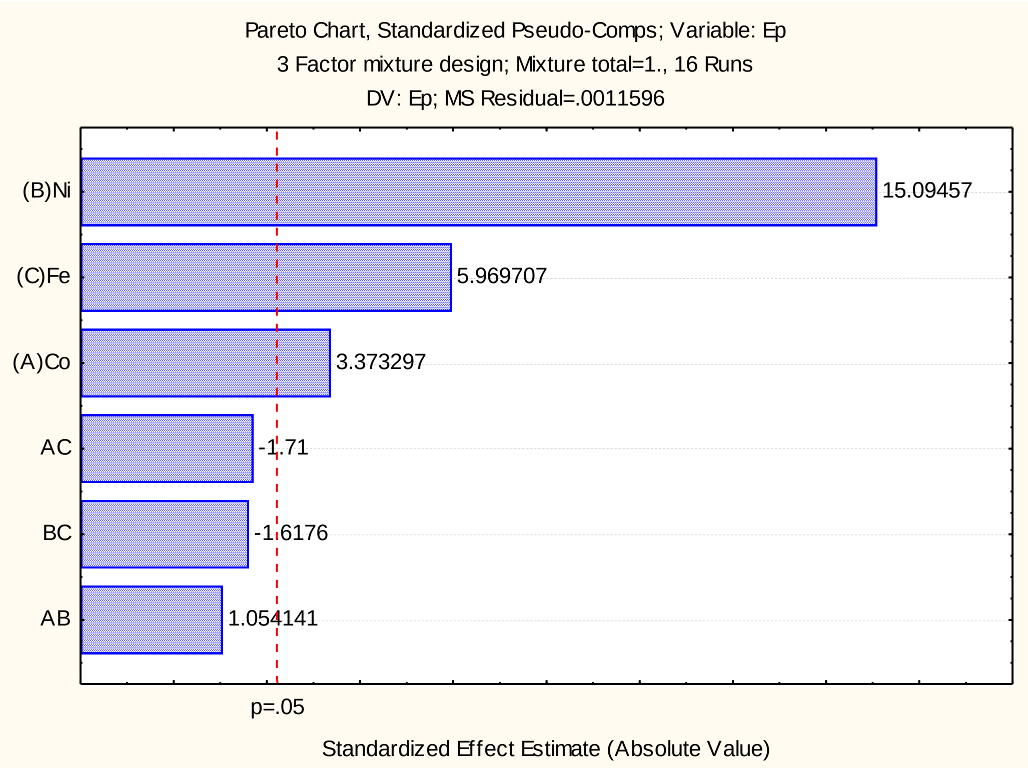

Figure S52. Pareto chart of E_p

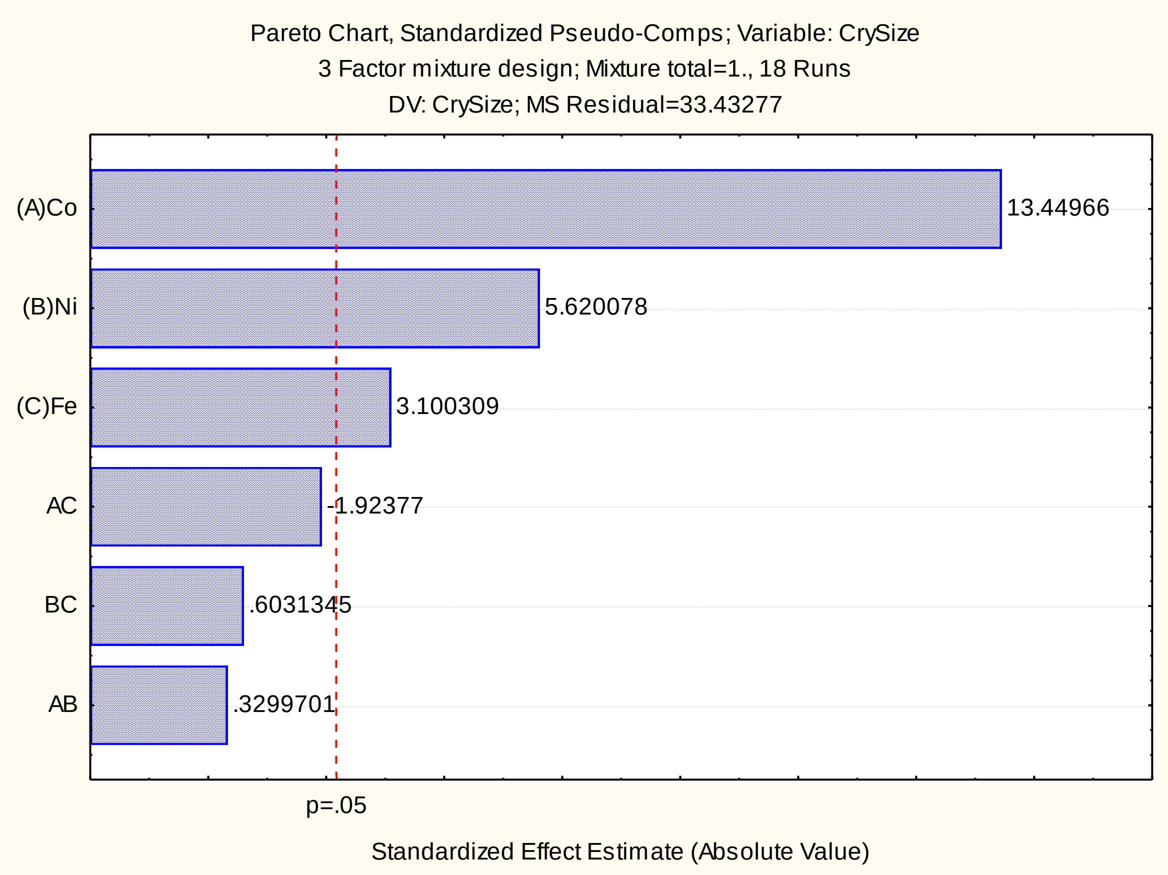

Figure S53. Pareto chart of crystal size

Surfaces theoretical model

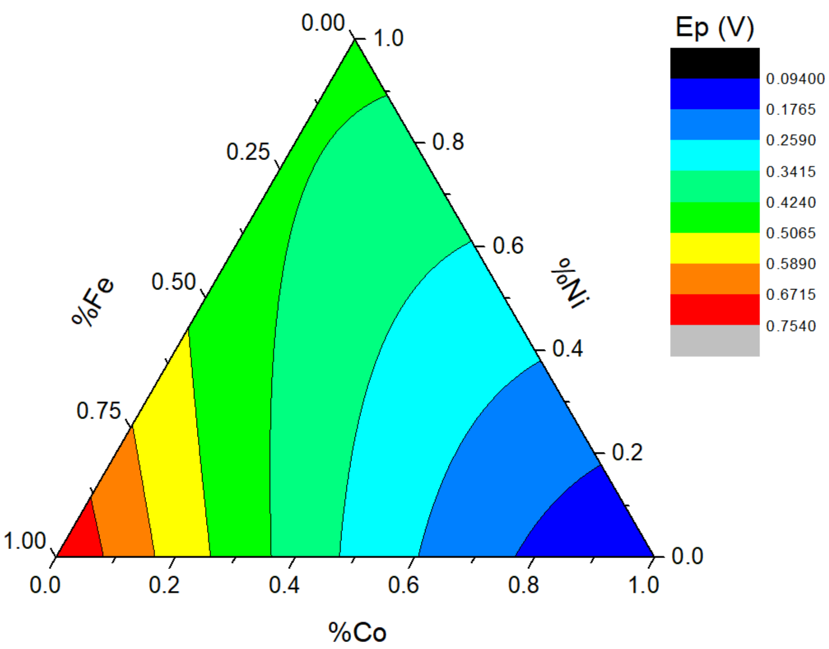

Figure S54. Peak potential response surface

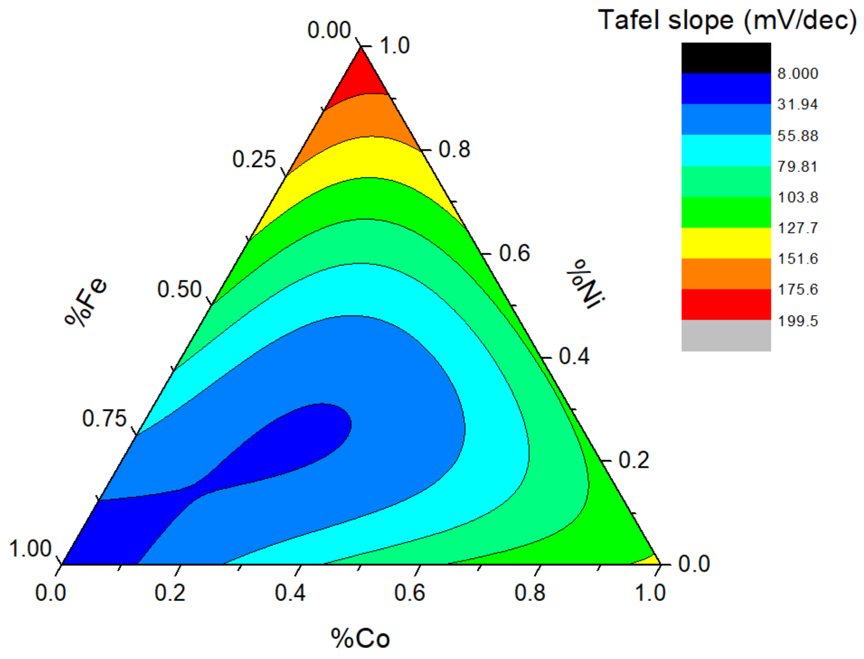

Figure S455. Tafel slope response surface

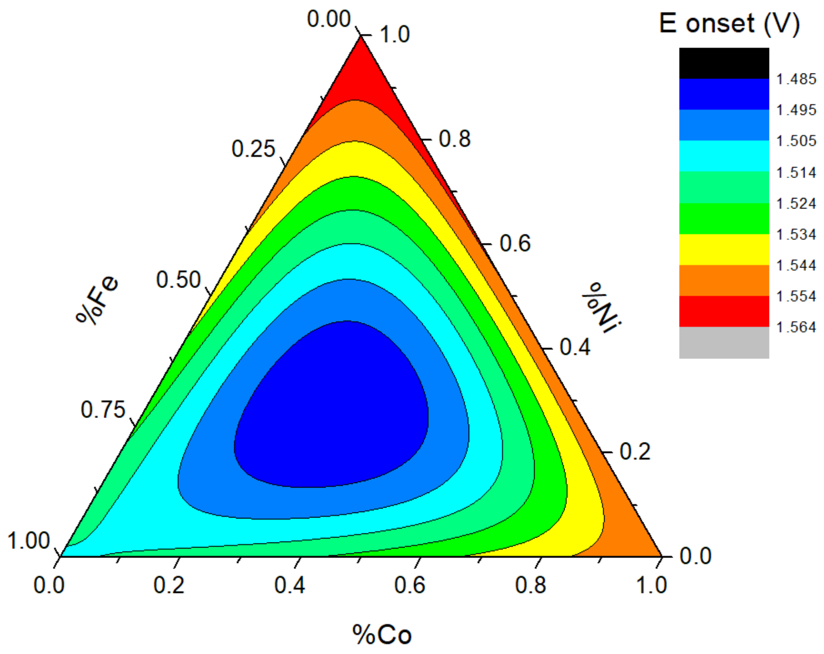

Figure S466. Onset potential response surface

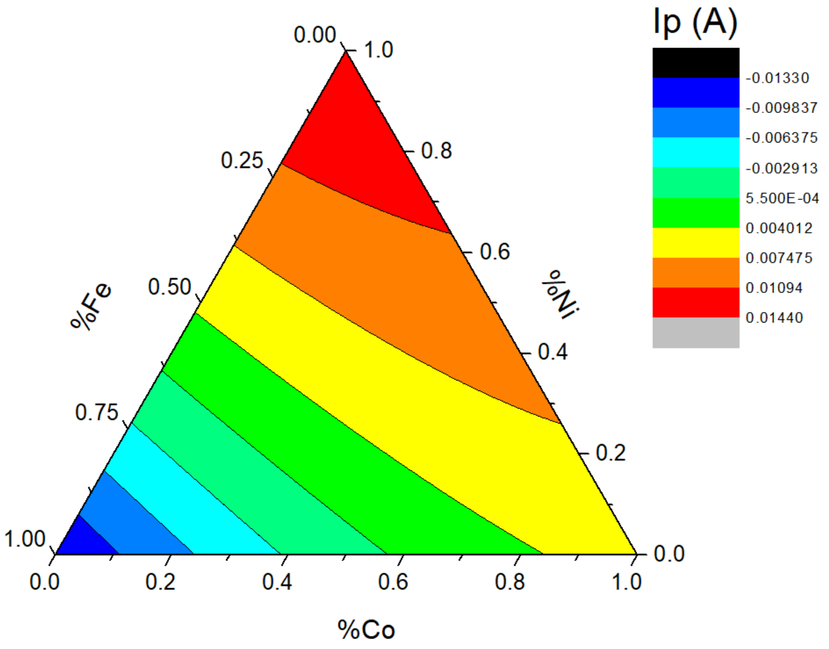

Figure S477. Peak current response surface

Tables with observed and predicted data of validation points

Table S4. Observed and predicted data of validation points for Tafel slope.

Tafel Slope

Validation point	Fract Co	Fract Ni	Fract Fe	Obs	Pred	+/-	%err
V1	0.330	0.330	0.340	35.870	55	41	75
V2	0.670	0.165	0.165	42.000	81	28	34
V3	0.165	0.670	0.165	144.760	125	28	22
V4	0.165	0.165	0.670	71.870	52	34	66

Table S5. Observed and predicted data of validation points for onset potential.

E_OnSet

Validation point	Fract Co	Fract Ni	Fract Fe	Obs	Pred	+/-	%err
V1	0.330	0.330	0.340	1.492	1.48	0.02	1.35
V2	0.670	0.165	0.165	1.492	1.51	0.02	1.33
V3	0.165	0.670	0.165	1.517	1.52	0.02	1.32
V4	0.165	0.165	0.670	1.511	1.50	0.02	1.33

Table S6. Observed and predicted data of validation points for peak current.

			Ip				
Validation point	Fract Co	Fract Ni	Fract Fe	Obs	Pred	+/-	%err
V1	0.333	0.333	0.333	0.003	0.0046	0.002	44
V2	0.670	0.165	0.165	0.003	0.0050	0.002	40
V3	0.165	0.670	0.165	0.013	0.0097	0.002	21
V4	0.165	0.165	0.670	0.001	-0.0007	0.004	-

Table S7. Observed and predicted data of validation points for peak potential.

			Ep				
Validation point	Fract Co	Fract Ni	Fract Fe	Obs	Pred	+/-	%err
V1	0.330	0.330	0.340	0.382	0.354	0.033	9
V2	0.165	0.670	0.165	0.421	0.394	0.037	9
V3	0.170	0.170	0.660	0.458	0.498	0.081	16
V4	0.670	0.165	0.165	0.258	0.219	0.030	14

Table S8. Observed and predicted data of validation points for crystal size.

			Crystal Size				
Validation point	Fract Co	Fract Ni	Fract Fe	Obs	Pred	+/-	%err
V1	0.330	0.330	0.340	41.446	42.782	5.300	12
V2	0.670	0.165	0.165	49.274	48.931	5.021	10
V3	0.165	0.670	0.165	34.245	38.182	5.021	13
V4	0.165	0.165	0.670	56.135	44.947	10.229	23

EIS investigation of Co60Ni20Fe20

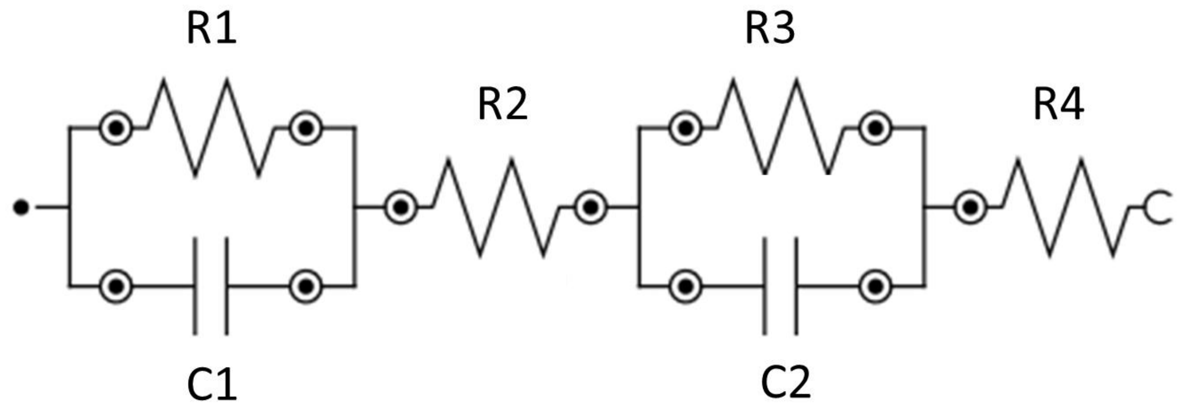

Figure S488. Equivalent circuit used to fit the data recorded during the experiments of electrochemical impedance spectroscopy

Table S9. Parameters obtained by the fitting of data recorded during the experiments of electrochemical impedance spectroscopy

E (V vs RHE)	C1 (F)	R1 (Ω)	R2(Ω)	C2(F)	R3(Ω)	R4(Ω)
1.367	0.106	1.01	0.001	0.088	101	2.106
1.418	0.117	0.932	0.001	0.0955	90.39	2.096
1.447	0.112	0.939	0.001	0.0984	33.49	2.1
1.459	0.1	0.782	0.001	0.105	9.55	2.091
1.469	0.0786	0.285	0.001	0.0984	2.524	2.081
1.507	0.0913	1.45	0.001	0.0758	0.15	2.1
1.552	0.0892	0.54	0.001	0.0626	0.0601	2.087

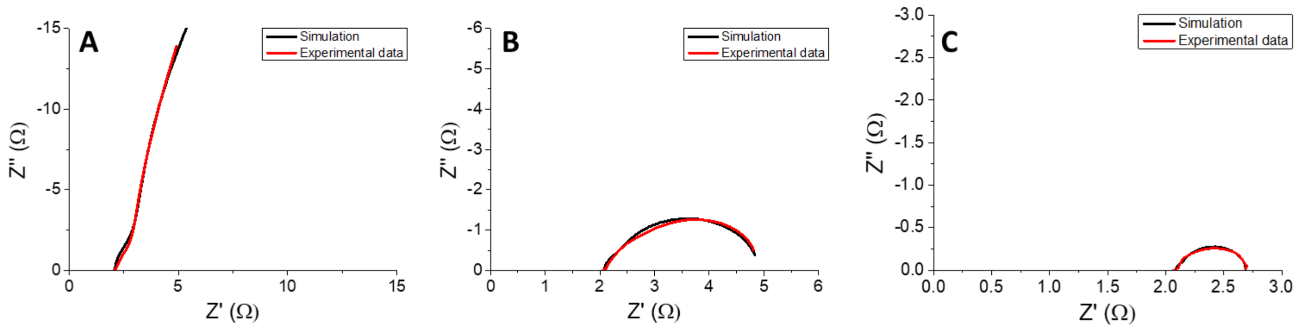

Figure S499. Comparison between experimental and simulated Nyquist plot at 1.367, 1.469 and 1.552 V vs RHE.

Paragraph S1. Chemometric models used

The equations tested to develop the proposed models, following the literature, are these:

1. Linear model

$$E(y) = \sum_{i=1}^{q} \beta_i x_i$$

For example: $y = \beta_1 * x_1 + \beta_2 * x_2 + \beta_3 * x_3$

2. Quadratic model

$$E(y) = \sum_{i=1}^{q} \beta_i x_i + \sum \sum_{i<j=2}^{q} \beta_{ij} x_i x_j$$

For example: $y = \beta_1 * x_1 + \beta_2 * x_2 + \beta_3 * x_3 + \beta_{12} * x_1 * x_2 + \beta_{13} * x_1 * x_3 + \beta_{23} * x_2 * x_3$

3. Full Cubic

$$E(y) = \sum_{i=1}^{q} \beta_i x_i + \sum \sum_{i<j=2}^{q} \beta_{ij} x_i x_j + \sum \sum_{i<j=2}^{q} \delta_{ij} x_i x_j (x_i - x_j) + \sum \sum \sum_{i<j<k=3}^{q} \beta_{ijk} x_i x_j x_k$$

For example: $y = \beta_1 * x_1 + \beta_2 * x_2 + \beta_3 * x_3 + \beta_{12} * x_1 * x_2 + \beta_{13} * x_1 * x_3 + \beta_{23} * x_2 * x_3 + \delta_{12} * x_1 * x_2 * (x_1 - x_2) + \delta_{13} * x_1 * x_3 * (x_1 - x_3) + \delta_{23} * x_2 * x_3 * (x_2 - x_3) + \beta_{123} * x_1 * x_2 * x_3$

4. Special Cubic

$$E(y) = \sum_{i=1}^{q} \beta_i x_i + \sum \sum_{i<j=2}^{q} \beta_{ij} x_i x_j + \sum \sum \sum_{i<j<k=3}^{q} \beta_{ijk} x_i x_j x_k$$

For example: $y = \beta_1 * x_1 + \beta_2 * x_2 + \beta_3 * x_3 + \beta_{12} * x_1 * x_2 + \beta_{13} * x_1 * x_3 + \beta_{23} * x_2 * x_3 + \beta_{123} * x_1 * x_2 * x_3$